JOURNAL

OF THE AMERICAN CHEMICAL SOCIETY

VOLUME 104, NUMBER 16 AUGUST 11, 1982

Magnetic Circular Dichroism Studies. 60.[1a] Substituent-Induced Sign Variation in the Magnetic Circular Dichroism Spectra of Reduced Porphyrins. 1.[1b] Spectra and Band Assignments

Joseph D. Keegan, Alan M. Stolzenberg, Yu-Cheng Lu, Robert E. Linder,[2] Günter Barth, Albert Moscowitz,*[3b] Edward Bunnenberg, and Carl Djerassi*[3a]

Contribution from the Departments of Chemistry, Stanford University, Stanford, California 94305, and The University of Minnesota, Minneapolis, Minnesota 55455.
Received October 21, 1981

Abstract: The magnetic circular dichroism (MCD) spectra of a number of unsubstituted, alkyl-substituted, and tetraphenyl-substituted chlorins, bacteriochlorins, and isobacteriochlorins are reported. In contrast to previous expectations, whether a "normal" or "inverted" MCD band sign pattern is observed in the chlorin series depends on the specific substituents at the periphery and at the center of the macrocycle. Substituent-induced MCD sign variation is also found in the isobacteriochlorin series. The sign pattern is invariant (inverted) in bacteriochlorin derivatives. New assignments for the location of the Q_0^x transition are made for a number of reduced porphyrin derivatives with MCD spectroscopy.

A wide variety of derivatives of the porphine chromophore (Figure 1, **1a**) play essential roles in the functioning of a number of biological systems. Pyrrole-substituted derivatives of iron porphine (**1b**), most notably iron protoporphyrin IX, serve in the transport or storage (hemoglobin and myoglobin) of dioxygen,[4a] in the transfer of electrons (cytochrome *c*),[4b] and in the metabolism of a variety of substrates (cytochrome P-450).[4c] Derivatives of magnesium chlorin (**2b**) and magnesium bacteriochlorin (**3b**), the chlorophylls and bacteriochlorophylls, are central to the light-gathering and energy-transducing systems in green plants[5a] and bacteria.[5b] Several chlorins are also involved in nonphotosynthetic processes. Bonellin (**5a**), as unusual chlorin which occurs without a complexed metal ion, is the physiologically active pigment of the marine echurian worm *Bonellia viridis*.[6] An iron chlorin, heme d_1,[7] is part of the electron-transfer system of *Pseudomonas* cytochrome oxidase.[8] Recently, a different iron chlorin, determined to be a catalase, has been isolated from *Neurospora crassa*.[9] Finally, the isobacteriochlorin chromophore (**4a**) is represented in nature in the form of a complex with iron (**4b**) as the prosthetic group of both sulfite and nitrite reductase[10] and in its metal-free form as an intermediate in the biosynthesis of vitamin B_{12}.[11]

Magnetic circular dichroism (MCD) has been extensively employed in studies of porphyrins and heme proteins. The applications which include component identification in microparticulate preparations, spin-state analysis, and the generation of molecular parameters for testing the validity of molecular orbital calculations have been reviewed recently by Sutherland,[12a] Holmquist,[12b] and Sutherland and Holmquist.[12c] In contrast, there have been many fewer MCD investigations of chlorin,[13] bacteriochlorin,[14a] and isobacteriochlorin[14b] derivatives. The first study[13a] of a series of

(1) (a) For Part 59, see: Keegan, J. D.; Stolzenberg, A. M.; Lu, Y.-C.; Linder, R. E.; Barth, G.; Bunnenberg, E.; Djerassi, C.; Moscowitz, A. *J. Am. Chem. Soc.* **1981**, *103*, 3201–3203. (b) Part 2 is the following paper in this issue.

(2) Surface Science Laboratory, 4151 Middlefield Road, Palo Alto, California 94303.

(3) (a) Stanford University. (b) University of Minnesota.

(4) (a) Ten Eyck, L. F. In "The Porphrins", Dolphin, D., Ed.; Academic Press: New York, 1979; Vol. VII, pp 445–472. (b) Ferguson-Miller, S.; Brautigan, D. L.; Margoliash, E. *Ibid.* pp 149–240. (c) Griffin, B. W.; Peterson, J. A.; Estabrook. R. W. *ibid.* pp 333–375.

(5) (a) Barber, J. "Primary Processes of Photosynthesis"; Elsevier: New York, 1977. (b) Clayton, R. K.; Sistrom, W. R. "The Photosynthetic Bacteria"; Plenum Press: New York, 1978.

(6) Ballantine, J. A.; Psaila, A. F.; Pelter, A.; Murray-Rust, P.; Ferrito, V.; Schembri, P.; Jaccarini, V. *J. Chem. Soc., Perkin Trans. 1* **1980**, 1080–1089.

(7) Barrett, J. *Biochem. J.* **1956**, *64*, 626–639.

(8) Blatt, Y.; Pecht, I. *Biochemistry* **1979**, *18*, 2917–2922.

(9) Jacob, G. S.; Orme-Johnson, W. H. *Biochemistry* **1979**, *18*, 2967–2980.

(10) (a) Siegal, L. M.; Murray, M. J.; Kamin, H. *J. Biol. Chem.* **1973**, *248*, 251–264. (b) Murphy, M. J.; Siegel, L. M.; Kamin, H.; Rosenthal, D. *Ibid.* **1973**, *248*, 2801–2814. (c) Murphy, M. J.; Siegel, L. M.; Toue, S. R.; Kamin, H. *Proc. Natl. Acad. Sci. U.S.A.* **1974**, *71*, 612–616. (d) Vega, J. M.; Garrett, R. H.; Siegel, L. M. *J. Biol. Chem.* **1975**, *250*, 7980–7989. (e) Vega, J. M.; Kamin, H. *Ibid.* **1977**, *252*, 896–909.

(11) (a) Scott, A. I.; Irwin, A. J.; Siegel, L. M.; Schoolery, J. N. *J. Am. Chem. Soc.* **1978**, *100*, 7987–7994. (b) Battersby, A. R.; McDonald, D.; Morris, H. R.; Thompson, M.; Williams, D. C.; Bykhovsky, V. Y.; Zaitseva, N. I.; Bukin, V. N. *Tetrahedron Lett.* **1977**, *2217*–2220.

(12) (a) Sutherland, J. C. In "The Porphyrins", Dolphin, D., Ed.; Academic Press: New York, 1978; Vol. III, pp 225–248. (b) Holmquist, B. *Ibid.* pp 249–270. (c) Sutherland, J. C.; Holmquist, B. *Annu. Rev. Biophys. Bioeng.* **1980**, *9*, 293–326.

0002-7863/82/1504-4305$01.25/0

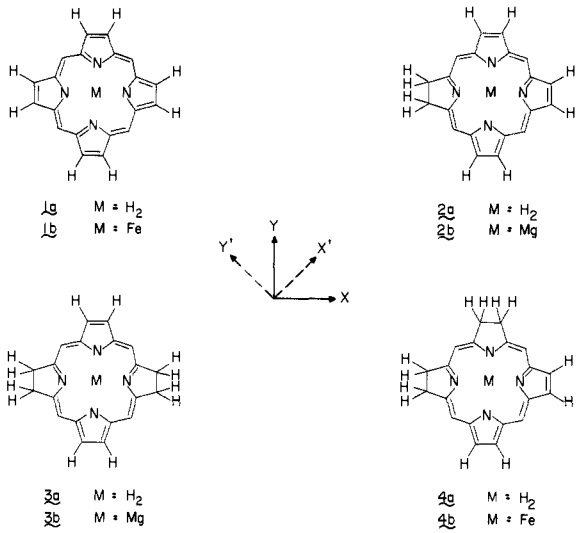

Figure 1. Structures of the porphine (**1**), chlorin (**2**), bacteriochlorin (**3**), and isobacteriochlorin (**4**) macrocycles. The x axis (solid line) is taken as the proton axis for porphine and the reduction axis for chlorin and bacteriochlorin. For isobacteriochlorin the symmetry axes are rotated by 45°.

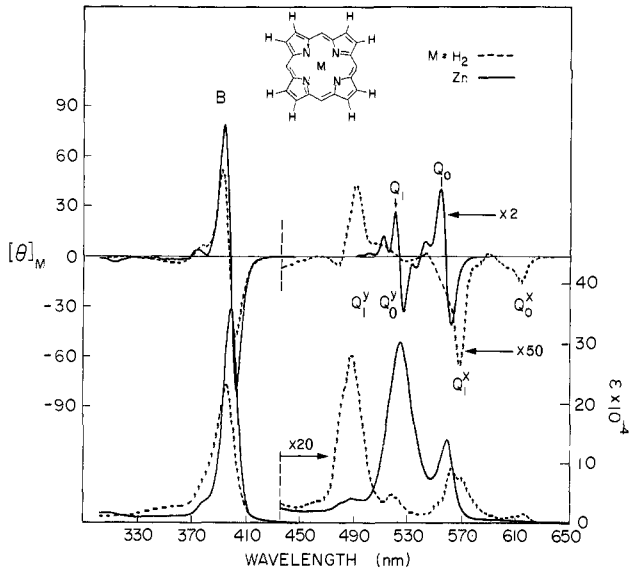

Figure 2. MCD and absorption spectra of porphine (- - -) and zinc porphine (—) in benzene.

substituted chlorins pointed to the usefulness of MCD for detecting very weak electronic transitions (the chlorin Q_0^x band), demonstrated that the intensities of some of the chlorin MCD bands were very sensitive to changes in the peripheral substituents, and constituted one of the first examples of a substituent-induced (the "chlorin" perturbation) inversion in the signs of the MCD bands of a cyclic π-electron system. The MCD spectrum of free-base

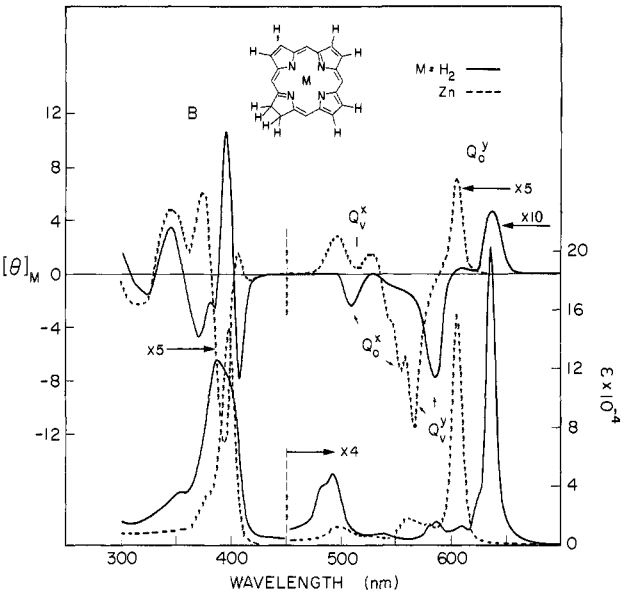

Figure 3. MCD and absorption spectra of chlorin (—) and zinc chlorin (- - -) in benzene.

chlorin (**2a**) (Figure 3) illustrates the phenomenon of sign inversion. In this spectrum the MCD bands associated with the two lowest-energy electronic transitions (Q_0^y and Q_0^x) have positive and negative signs, respectively. In the spectrum of the parent chromophore, free-base porphine (**1a**) (Figure 2), the corresponding MCD bands, Q_0^x and Q_0^y, respectively, have negative and positive signs.

Several efforts have been made to provide a firm theoretical basis for the occurrence of sign inversions in porphyrin derivatives. McHugh et al.[15] attempted to calculate the MCD signs of porphyrins and reduced porphyrins by the SCMO-PPP-CI method, whereas Kaito et al.,[16] within the same approximation, but with Löwdin orthogonalized AO's, were successful in calculating the MCD sign inversions of a carbonyl-substituted porphyrin. Unfortunately, numerical calculations such as these must be carried out explicitly for each porphyrin derivative under consideration. Thus, they lack easily generalizable predictive power for spectra–structure correlations and accessibility to most porphyrin chemists. Recently, Michl[17] has presented a very useful theoretical formulation which relates the absolute MCD signs of the four lowest-energy electronic transitions of systems derivable from a $(4N + 2)$-electron $[n]$annulene perimeter with their molecular structures. This approach should have considerable appeal to porphyrin chemists since it merely requires knowledge of the relative absolute size of the orbital energy differences between the two highest occupied (ΔHOMO) and two lowest unoccupied (ΔLUMO) molecular orbitals. Such knowledge is usually available when the framework of Gouterman's four-orbital model[18] for porphyrin states in conjunction with qualitative theoretical concepts[19] is used.

Michl explicitly predicted the MCD sign patterns of the unsubstituted porphine, chlorin, bacteriochlorin, and isobacteriochlorin chromophores and found support for the validity of his arguments from the MCD spectra reported for a number of substituted porphyrins and chlorins.[17a,b] In response to this challenge we initiated an experimental study of a number of unsubstituted and octaethyl- and tetraphenylchlorins, bacterio-

(13) (a) Briat, B.; Schooley, D. A.; Records, R.; Bunnenberg, E.; Djerassi, C. *J. Am. Chem. Soc.* **1967**, *89*, 6170–6177. (b) Houssier, C.; Sauer, K. *Ibid.* **1970**, *92*, 779–791. (c) Breton, J.; Hilaire, M. *C. R. Hebd. Seances Acad. Sci., Ser. D.* **1972**, *274*, 678–681. (d) Schreiner, A. F.; Gunter, J. D.; Hamm, D. J.; Jones, I. D.; White, R. C. *Inorg. Chim. Acta* **1978**, *26*, 151–155. (e) Janzen, A. F.; Bolton, J. R.; Stillman, M. J. *J. Am. Chem. Soc.* **1979**, *101*, 6337–6341. (f) Orii, Y.; Shimada, H.; Nozawa, T.; Hatano, M. *Biochem. Biophys. Res. Commun.* **1977**, *76*, 983–988. (g) Vickery, L. E.; Palmer, G.; Wharton, D. C. *Ibid.* **1978**, *80*, 458–463. (h) Walsh, T. A.; Johnson, M. K.; Greenwood, C.; Barber, D.; Springall, J. P.; Thomson, A. J. *Biochem. J.* **1979**, *177*, 29–39. (i) Boxer, S. G.; Wright, K. A. *J. Am. Chem. Soc.* **1979**, *101*, 6791–6794.

(14) (a) Sutherland, J. C.; Olson, J. M. *Photochem. Photobiol.* **1981**, *33*, 379–384. (b) Stolzenberg, A. M.; Strauss, S. H.; Holm, R. H. *J. Am. Chem. Soc.* **1981**, *103*, 4763–4778.

(15) McHugh, A. J.; Gouterman, M.; Weiss, C. *Theor. Chim. Acta* **1972**, *24*, 346–370.

(16) Kaito, A.; Nozawa, T.; Yamamoto, T.; Hatano, M.; Orii, Y. *Chem. Phys. Lett.* **1977**, *52*, 154–160.

(17) (a) Michl, J. *J. Am. Chem. Soc.* **197**[illegible]811. (b) *Ibid.* **1978**, *100*, 6812–6818. (c) *Ibid.* **1978**, *100*, 6819–6824.

(18) Gouterman, M. In "The Porphyrins", Dolphin, D.; Ed.; Academic Press: New York, 1978; Vol. III, pp 1–165.

(19) Dewar, M. J. S.; Dougherty, R. C. "The PMO Theory of Organic Chemistry"; Plenum Press: New York, 1975.

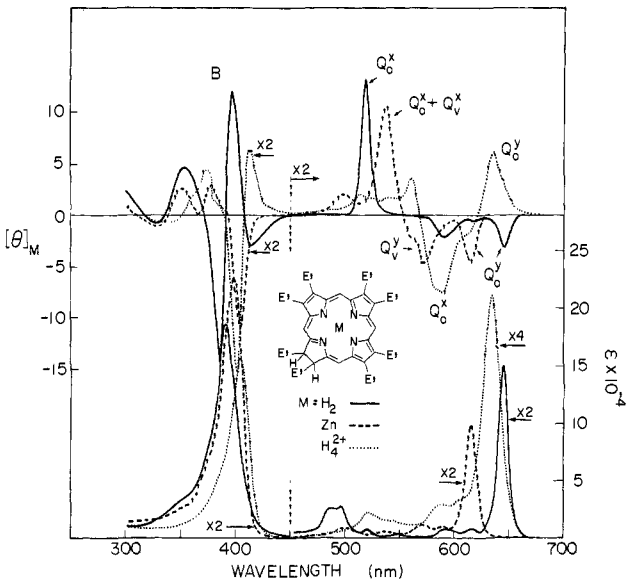

Figure 4. MCD and absorption spectra of octaethylchlorin (—) and zinc octaethylchlorin (- - -) in benzene. The spectra of octaethylchlorin dication (···) are in 0.1 N trifluoroacetic acid in benzene.

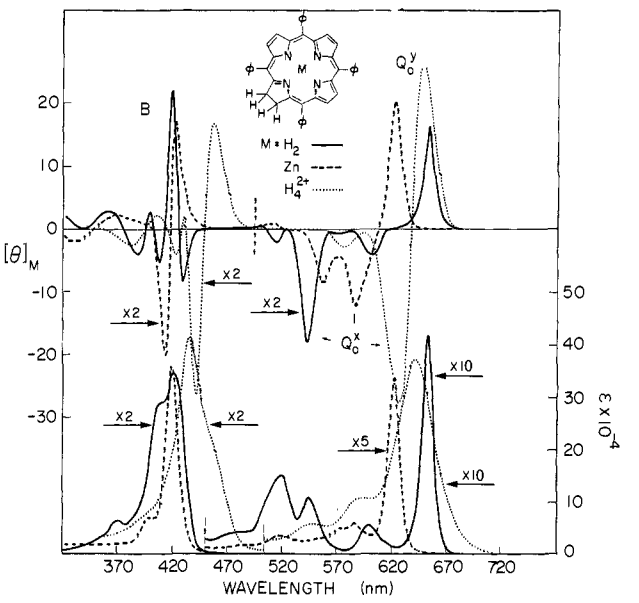

Figure 5. MCD and absorption spectra of tetraphenylchlorin (—) and zinc tetraphenylchlorin (- - -) in benzene. The spectra of tetraphenylchlorin dication (···) are in 0.1 N trifluoroacetic acid in benzene.

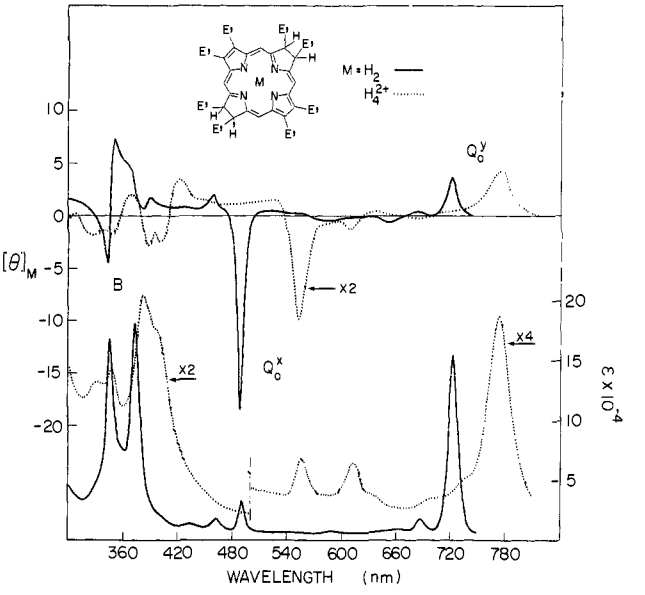

Figure 6. MCD and absorption spectra of octaethylbacteriochlorin (—) and octaethylbacteriochlorin dication (···) in benzene and 0.1 N trifluoroacetic acid in benzene, respectively.

chlorins, and isobacteriochlorins. Our early observation that the lowest-energy *electronic* MCD bands of zinc octaethylchlorin were not inverted, as would be expected by direct application of the tenents of Michl's perimeter model, indicated that the chlorin perturbation was not as traumatic as might be supposed and that the effects of peripheral substituents needed to be considered as well. The results of an elaboration of Michl's model required for alkyl-, phenyl-, and carbonyl-substituted zinc chlorins have been presented in preliminary form.[1a]

In Part 1 of this series we present our experimental data for chlorins, bacteriochlorins, and isobacteriochlorins, make assignments for the location of the Q_0^x transition throughout the series, point out instances of substituent-induced sign inversion within each series, and comment on the ability of the four-orbital model to represent the Soret band. In Part 2[1b] we give the results of the substituent perturbation treatment required to rationalize and predict the MCD band sign patterns of the reduced porphyrins and show that Michl's perimeter model[17] can be used for MCD spectra–structure correlations with a remarkable degree of success.

Experimental Section

Porphine was purchased from Sigma and purified by chromatography prior to use. Chlorin was synthesized from 2-((dimethylamino)-methyl)pyrrole by the high-temperature sealed-tube modification[20] of the Eisner and Linstead[21] procedure. Chlorin was isolated from the reaction mixture by chromatography over alumina followed by conversion to the zinc complex and further chromatography on silica to remove small traces of porphine. The Egorova et al.[20] modification also produces bacteriochlorin and isobacteriochlorin; however, owing to their extreme sensitivity to oxidation by atmospheric oxygen, no attempt was made to isolate them.

Octaethylporphyrin was prepared according to the procedure of Cheng and LeGoff.[22] *trans*-Octaethylchlorin was synthesized from iron(II) octaethylporphyrin by the sodium/isoamyl alcohol method of Whitlock et al.[23] The modifications to this dissolving metal procedure needed to maximize the yield of the two all-trans isomers of octaethylisobacteriochlorin have been described by one of us.[24] The reaction product also contained octaethylbacteriochlorin which was isolated by medium-pressure liquid chromatography over magnesium oxide.

Tetraphenylporphyrin was prepared from pyrrole and benzaldehyde by the procedure of Alder et al.[25] and freed from the tetraphenylchlorin impurity by treatment with 2,3-dichloro-5,6-dicyanobenzoquinone.[26] Tetraphenylchlorin and tetraphenylbacteriochlorin were obtained by the diimide reduction of tetraphenylporphyrin when the procedure of Whitlock et al.[23] was followed, and zinc tetraphenylchlorin was the precursor for tetraphenylisobacteriochlorin when the same reduction method was used.

Zinc was inserted with use of the dimethylformamide procedure of Alder et al.[27] or the zinc acetate/methanol method described by Fuhrhop and Smith.[28] The zinc complex of octaethylbacteriochlorin could not be prepared. Since all of the reduced prophyrins studied are subject to photooxidative degradation or else to oxidation to a more highly unsaturated derivative, special care was taken to minimize exposure of the compounds to both light and oxygen.

(20) Egorova, G. D.; Solov'ev, K. N.; Shul'ga, A. M. *Zh. Obshch. Khim.* **1967**, *37*, 357–361.
(21) Eisner, U.; Linstead, R. P. *J. Chem. Soc.* **1955**, 3742–3749.
(22) Cheng, D. O.; LeGoff, E. *Tetrahedron Lett.* **1977**, *1469*–1472.
(23) Whitlock, H. W.; Hanauer, R.; Oester, M. Y.; Bower, B. K. *J. Am. Chem. Soc.* **1969**, *91*, 7485–7489.
(24) Stolzenberg, A. M.; Spreer, L. O.; Holm, R. H. *J. Am. Chem. Soc.* **1980**, *102*, 364–370.
(25) Adler, A. D.; Longo, F. R.; Finarelli, J. D.; Goldmacher, J.; Assour, J.; Korsakoff, L. *J. Org. Chem.* **1967**, *32*, 476.
(26) Barnett, G. H.; Hudson, M. F.; Smith, K. M. *Tetrahedron Lett.* **1973**, 2887–2888.
(27) Adler, A. D.; Longo, F. R.; Kampas, F.; Kim, J. *J. Inorg. Nucl. Chem.* **1970**, *32*, 2443–2445.
(28) Fuhrhop, J. H.; Smith, K. M. In "Porphyrins and Metalloporphyrins", Smith, K. M., Ed.; Elsevier: New York, 1975; p 798.

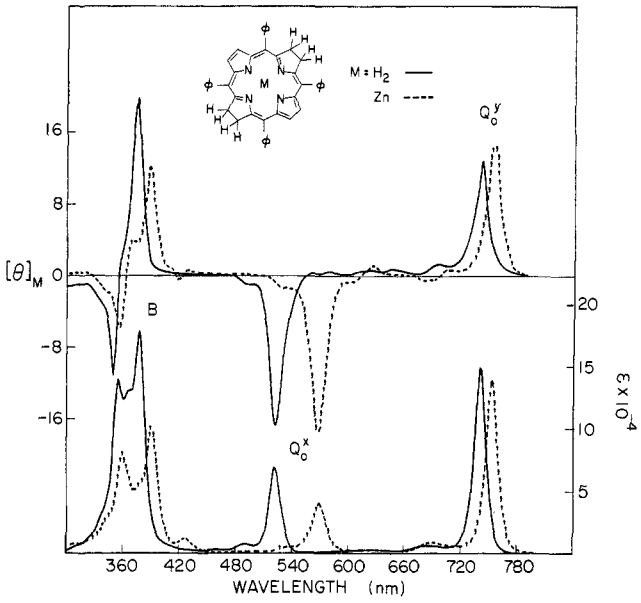

Figure 7. MCD and absorption spectra of tetraphenylbacteriochlorin (—) and zinc tetraphenylbacteriochlorin (- - -) in benzene.

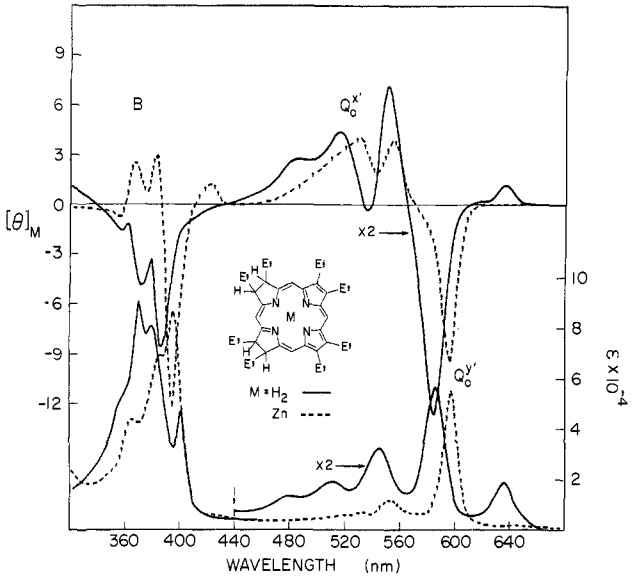

Figure 8. MCD and absorption spectra of octaethylisobacteriochlorin (—) and zinc octaethylisobacteriochlorin (- - -) in benzene.

The solvents used for spectroscopy, benzene or toluene, were of spectroscopic quality and were distilled from sodium metal under a stream of nitrogen or argon just prior to use. Dications were formed by dissolving the free bases in a 0.1 N solution of trifluoroacetic acid in benzene. The solvent system used to prepare the dianions from the neutral species was a mixture of dimethyl sulfoxide–toluene–water (8:1:1 v/v/v) whose sodium hydroxide concentration was 0.02 N. EPA (diethyl ether–isopentane–ethanol, 5:5:2 v/v/v) was used as the solvent for MCD measurements at 77 K. MCD measurements were made with a JASCO Model J-40 circular dichrometer equipped with a 15 kG electromagnet. A Cary 14M spectrophotometer was used for absorption spectral measurements. Both instruments were interfaced to a Data General NOVA 840 computer for data acquisition. Instrument calibration procedures have been previously reported.[29] Molar magnetic ellipticities, $[\theta]_M$, are reported in the units deg cm^2 dmol^{-1} G^{-1}. Selected MCD and absorption spectra are presented in Figures 2–10 and spectral data are summarized in Table I.

Results and Discussion

Absorption and MCD Spectra Characteristics. In Gouterman's four-orbital model[18,30] the low-lying ($\pi\pi^*$) excited states of D_{4h}

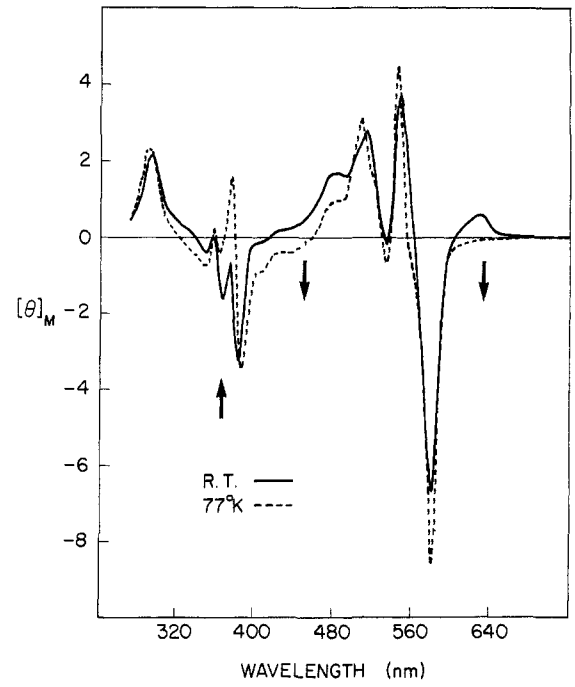

Figure 9. MCD spectra of octaethylisobacteriochlorin in EPA at room temperature (—) and at 77 K (- - -).

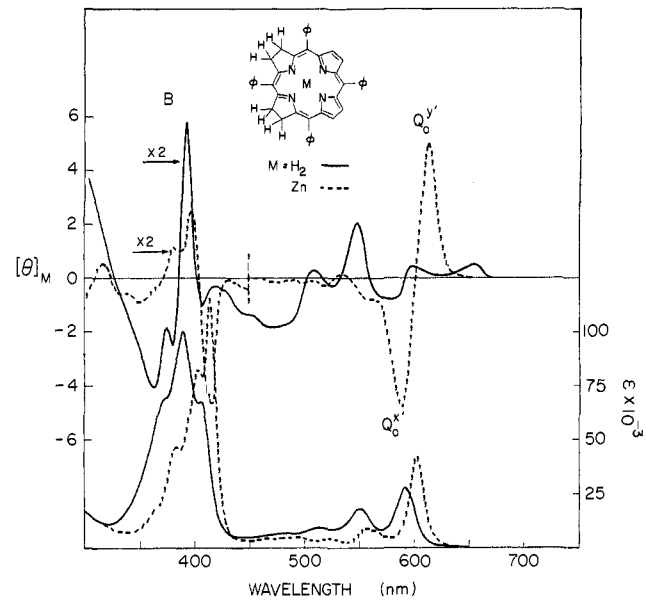

Figure 10. MCD and absorption spectra of tetraphenylisobacteriochlorin (—) and zinc tetraphenylisobacteriochlorin (- - -) in benzene.

porphyrins are considered to arise from single electron excitations from the two highest occupied molecular orbitals (HOMO's) to the two lowest unoccupied molecular orbitals (LUMO's). The latter two orbitals, e_g1 and e_g2 (see, for example, the energy level diagram for porphine dianion in Figure 3 of part 2[1b]) are degenerate by symmetry, whereas the former two, the a_{1u} and a_{2u} orbitals, are taken to be almost degenerate. Pairwise interaction between the almost degenerate singlet excited configurations, $^1(a_{2u}e_g)$ and $^1(a_{1u}e_g)$, results in minus and plus states in which the equal transition dipoles cancel or reinforce each other. This gives rise to the weak and strong transitions in the visible and UV regions, respectively, evident in the absorption spectrum of zinc porphine shown in Figure 2. In the more general notation of Platt for cyclic π-electron systems, these bands would be referred to

(29) Barth, G.; Dawson, J. H.; Dolinger, P. M.; Linder, R. E.; Bunnenberg, E.; Djerassi, C. *Anal. Biochem.* **1975**, *65*, 100–108.

(30) (a) Gouterman, M. *J. Mol. Spectrosc.* **1961**, *6*, 138–163. (b) Gouterman, M.; Wagnière, G. H.; Snyder, L. C. *Ibid.* **1963**, *11*, 108–127.

as the L and B bands; however, in porphyrins the commonly used notation is Q_0 and Soret (or B). We adopt the latter system throughout. The other bands are either of vibronic origin or else arise from transitions to higher states not considered in the four-orbital model. On formation of the free base, the symmetry of the porphyrin is lowered from D_{4h} to D_{2h} and the Q and B states are no longer degenerate. As shown in the absorption spectrum of porphine free base in Figure 2, the splitting in the visible Q_0^x and Q_0^y transitions is appreciable, whereas no evidence of splitting is observed in the Soret region. A number of calculations,[18] e.g., the ab initio calculations on porphine and magnesium porphine of Petke et al.,[31] support the four-orbital model for the Q bands of D_{4h} and D_{2h} porphyrins. The Soret band is described less well by the four-orbital model in both cases.

The MCD that may be associated with any particular electronic transition, a $\rightarrow$ j, of an isotropic sample is described[32] by the expression

$$[\theta]_M = -21.3458\{f_1A + f_2[B + C/kT]\} \quad (1)$$

where $[\theta]_M$ is the molar magnetic ellipticity in the units already denoted, f_1 and f_2 are line-shape functions, and A (in $D^2\beta_e$), B, and C/kT (both in the units $D^2\beta_e/cm^{-1}$) are the Faraday parameters of the transition. The C term will be nonzero only if the initial state a is degenerate. Consequently, only the A and B parameters are of interest for the porphyrin derivatives considered here.

The A term may be nonzero if the upper state j is degenerate. The magnetic field lifts the degeneracy of the excited states and the two formally degenerate states, j and j', are split by an energy which is small but proportional to the intensity of the magnetic field and the angular momentum of the excited state. For D_{4h} porphyrins, the lower-energy state of the degenerate pair selectively absorbs right circularly polarized light while the other state absorbs only left circularly polarized light. In the MCD spectrum, one then observes S-shaped (the line shape of the f_1 function) bands such as those found for the degenerate Q and B states of zinc porphine (Figure 2). The sign pattern of the MCD A-term bands associated with the Q_0 and B_0 transitions of zinc porphine is $-+-+$, with increasing energy, and is referred to as the "normal" sign pattern. It will also be noted in Figure 2 that one of the A terms in the Q_1 region of zinc porphine is inverted. Such vibronically induced sign inversions have been treated by us in some detail elsewhere.[33]

For porphyrin derivatives of symmetry lower than D_{4h}, e.g., free-base porphyrins, the structural perturbation has lifted the excited-state degeneracies and only the B term in the expression given above may be nonzero. B terms arise from the mixing of two or more nondegenerate states by the external magnetic field.[34] The consequence of this mixing is that these states will exhibit preferential absorption for either left or right circularly polarized light. In porphine free base (Figure 2) the orthogonally polarized Q_0^x and Q_0^y transitions are well separated. The negative sign of the MCD associated with the Q_0^x transition indicates that this state absorbs more right than left circularly polarized light; conversely, the Q_0^y state absorbs more left than right circularly polarized light. Thus, in general, the shape function, f_2, of the B term will be that of an absorption band. When the two states, not degenerate by symmetry, are not well separated, as is the case for the B_0^x and B_0^y states of porphine free base, the MCD band shape will have an S shape similar to that of an A term. The sign pattern of the B-term MCD bands associated with the lowest-energy electronic transitions of porphine free base is $-+-+$ with increasing energy. This pattern is defined as the "normal" B-term MCD band sign pattern for low-symmetry porphyrin derivatives.

In subsequent sections, and in Part 2,[1b] we will consider the absorption and MCD spectra of reduced porphyrins in some detail; consequently, our prefatory comments here are brief. In the four-orbital picture[18,30] of porphin electronic states the saturation of one or more ethylenic double bonds on the periphery lifts the accidental degeneracy of the HOMO's as well as the symmetry-dictated degeneracy of the LUMO's. The manner of the splitting depends on the number and arrangement of the chlorin perturbations as is illustrated in Figures 3–5 and 9 of Part 2. When the energy-level diagram for chlorin dication (Figure 4, Part 2) is used as a specific example, it can be noted that the y-polarized transitions (so labeled because of the conventional choice of axes shown in Figure 1 of this work) differ greatly in energy, whereas the x-polarized transitions are more nearly degenerate. This situation gives rise in the four-orbital model to a moderately strong low-energy transition, labeled Q_0^y; to a much weaker transition, labeled Q_0^x, which is usually well separated from the Q_0^y transition; and to two more intense, but less well separated, transitions (B_0^x and B_0^y) that together contribute to the envelope of the Soret absorption band. These are the transitions which are indicated in the spectra of the chlorin derivatives shown in Figures 3–5. A similar picture, but different in detail, obtains from the four-orbital model for the other reduced porphyrins. In contrast to the normal ($-+-+$) MCD band sign pattern found for the electronic transitions of the vast majority of perimeter symmetric porphyrins, we will have may occasions in subsequent sections to refer to the "inverted" ($+-$) sign pattern frequency found in the visible, but also in the Soret, regions of the MCD spectra of reduced porphyrins.

Finally, we emphasize that, in distinction to Michl's usual practice,[17] reference to the sign of an MCD band relates to the sign of $[\theta]_M$ in the band and not to the sign of the B term of the transition, unless specifically so noted.

Assignment of the Q_0^x Transition for Reduced Porphyrins. In Part 2 we will be concerned with the development of a protocol which can be used in conjunction with Michl's perimeter model[17] to relate the molecular structures of a variety of substituted reduced porphyrins with the sign patterns of the bands observed in their MCD spectra. Our attention there will focus primarily on the MCD associated with the low-energy Q_0^y and Q_0^x transitions and less on that in the Soret region. Consequently, since the Q_0^y transition of the reduced porphyrins is always relatively strong and easily identifiable, our principal concern here will be with the Q_0^x transition. We do, however, collect such polarization data as have been reported for the Soret transition of several of the reduced porphyrins and comment on the extent to which its composition is "four-orbital" in nature as judged by the results of recent ab initio calculations and by its appearance in the MCD spectrum.

In the following sections we make assignments first for the chlorins, then for the bacteriochlorins, and finally for the isobacteriochlorins. The chlorin section is presented in some detail since the presence of MCD bands of vibronic origin obscures simplistic MCD assignment protocols in a number of cases. Assignments are striaightforward in the bacteriochlorins for which sign variation within the series is not observed. Sign variation is again found in the isobacteriochlorin series, necessitating again a more careful treatment.

(i) **Chlorins.** Good reviews on the electronic structure and spectra of chlorins and chlorophylls have been given recently by Petke et al.,[35,36] and we refer the reader to them for a more complete exposition of transition assignments in both the visible and Soret regions. Our assignments for the location of the Q_0^x transition in the chlorins studied here are based on several con-

(31) Petke, J. D.; Maggiora, G. M.; Shipman, L. L.; Christoffersen, R. E. *J. Mol. Spectrosc.* **1978**, *71*, 64–84.

(32) (a) Schatz, P. N.; McCaffery, A. J. *Q. Rev., Chem. Soc.* **1969**, *23*, 552–583. (b) Stephens, P. J. *Annu. Rev. Phys. Chem.* **1974**, *25*, 201–232.

(33) (a) Linder, R. E.; Barth, G.; Bunnenberg, E.; Djerassi, C.; Seamans, L.; Moscowitz, A. *J. Chem. Soc., Perkin Trans. 2*, **1974**, 1712–1718. (b) Barth, G.; Linder, R. E.; Waespe-Sarcevic, N.; Bunnenberg, E.; Djerassi, C.; Aronowitz, Y. J.; Gouterman, M. *J. Chem. Soc., Perkin Trans. 2*, **1977**, 337–343.

(34) As indicated in eq 1, B terms may also overlay A terms associated with transitions to degenerate excited states, a situation covered in some detail in ref 12a, 15, and 17a.

(35) Petke, J. D.; Maggiora, G. M.; Shipman, L. M.; Christoffersen, R. E. *J. Mol. Spectrosc.* **1978**, *73*, 311–331.

(36) Petke, J. D.; Maggiora, G. M.; Shipman, L.; Christoffersen, R. E. *Photochem. Photobiol.* **1979**, *30*, 203–223.

Table I. MCD and Absorption Spectral Data for Reduced Porphyrins

compound	spectrum	solvent[c]	MCD:[a] $\lambda_{max}/[\theta]_M$; absorption:[b] $\lambda_{max}/10^{-3}\epsilon$													
			Soret region				$Q_v^{x\,d,e}$			Q_0^x		$Q_v^{y\,e}$			Q_0^y	
chlorin	MCD	B	372	387	397	408				510[f]		550 (s)	587	638		
			−4.6	−2.4	10.6	−7.6				−0.2		−0.1	−0.8	0.5		
	A	B	354 (s)	389	399 (s)		484	494		510 (s)		537	588	638		
			35.7	126.2	113.5		9.9	12.1		2.7		2.0	4.1	50.7		
octaethylchlorin	MCD	B	355	386	398	415				520			593	647		
			4.9	−13.5	12.4	−3.1				6.3			−1.0	−1.6		
	A	B	352 (s)	392			487	496		522			593	646		
			32.7	187.4			12.7	13.1		4.2			4.2	75.2		
bonellin dimethyl ester (5a)	MCD	B	351	387	399	412				521[f]			589	638		
			3.9	−7.5	14.2	−6.0				4.1			−1.1	−1.5		
	A	B	350 (s)	393			488	496		520			590	641		
			32.6	166.1			12.6	13.2		3.2			4.1	59.4		
tetraphenylchlorin	MCD	B	400	410	420	430			513	543[f]			601	653		
			2.1	−5.1	21.1	−8.2			−1.0	−8.9			−2.1	8.2		
	A	B	372	409 (s)	421				519	545			601	653		
			31.0	144.2	172.1				15.0	10.8			5.8	41.8		
zinc chlorin	MCD	B	347	375	393	408		497	529	555[f]	546 (s)		567	606		
			1.0	1.1	−2.5	0.3		0.6	0.4	−1.4	−0.6		−2.1	1.4		
	A	B	349 (s)	379 (s)	399			497	529			560		606		
			9.1	34.0	147.3			3.1	1.6			4.5		39.5		
zinc octaethylchlorin	MCD	B	352	378		406		502		538[g]	561 (s)	573		615		
			1.3	1.53		−5.5		1.0		5.2	−1.0	−2.4		−2.3		
	A	B	351 (s)	375 (s)		400		503		539	569	589		617		
			13.9	34.5		113.1		3.8		3.3	6.1	5.0		49.2		
zinc bonellin dimethyl ester (5b)	MCD	B	348	378	391	404		500		537[f,g]		561	574	611		
			1.0	2.1	1.2	−7.0		0.9		4.4		−1.5	−1.8	−1.4		
	A	B	349 (s)	376 (s)		402		500		538		568	584	612		
			14.2	34.2		134.2		4.7		3.8		7.0	6.1	47.7		
zinc rhodochlorin (6)	MCD	B	341	367	400	423		507		555[f]			599	646		
			−2.3	3.3	−6.6	7.1		0.6		−3.3			−2.2	5.1		
	A	B	361		402 (s)	418		508		557			599	646		
			24.7		78.9	104.1		3.5		2.6			9.1	62.9		
zinc tetraphenylchlorin	MCD	B	369	413	424			508	555	586				623		
			1.5	−10.2	8.7			1.0	−8.3	−12.0				20.1		
	A	B	369	401 (s)	420			514	554	586				622		
			17.9	67.3	354.6			6.7	6.3	11.9				67.1		
zinc chlorin	MCD	P	351	378	402	411		505	524	573[f]	554			609		
			1.2	0.9	−5.1	4.2		0.7	0.3	−6.0	−2.3			5.8		
	A	P		386	406			508	539	573				609		
				53.3	264.9			4.7	3.2	6.7				50.6		
zinc octaethylchlorin	MCD	P	386	395	406	416		510	549	566[f]		581		614	626[h]	
			1.7	−1.0	5.5	−8.3		1.3	3.9	−1.5		−4.4		−0.7	0.5	
	A	P	386 (s)			410		509	545		575		590	618		
			35.4			180.3		5.4	3.0		7.1		6.2	60.3		
zinc bonellin dimethyl ester (5c)	MCD	P	380	393	404	411		507	546	560 (s)[f]		575		616		
			2.1	(neg)	5.1	−6.9		0.8	2.1	−1.4		−3.7		1.4		
	A	P	387		410			510	543		572		584	615		
			42.9		182.1			4.9	3.1		6.7		6.3	45.6		
zinc tetraphenylchlorin	MCD	P	424	436				560		600[f]				626		
			−8.0	9.5				−5.0		−22.1				27.4		

	A	P	427					531	575			600				626	
			295.8					6.1	8.4			14.4				42.0	
chlorin dication	MCD	TFA	338	371	400	410			524			586[f]			604 (s)	627	
			−0.8	1.8	−13.1	8.2			0.3			−3.0			−0.6	3.5	
	A	TFA		385 (s)	403				517			577				626	
				61.8	149.3				3.1			4.4				26.3	
octaethylchlorin dication	MCD	TFA	335	375	401	414		515	560			587[f]			613 (s)	636	
			−0.3	2.3	−7.5	3.3		1.0	1.8			−3.8			−0.9	2.9	
	A	TFA		383 (s)	405			521				589			612 (s)	635	
				51.6	155.4			5.7				7.4			9.2	52.8	
bonellin dimethyl ester dication	MCD	TFA	340	374	402	415		520	559			587[f]			582 (s)	634	
(5d)			−1.0	1.2	−10.0	3.9		0.4	0.5			−1.7			0.3	1.6	
	A	TFA	368		405			521				585			606 (s)	633	
			30.6		187.0			4.7				6.4			7.5	38.5	
tetraphenylchlorin dication	MCD	TFA	404	422	441	458			576			622[f]				649	
			1.2	−2.2	−13.0	8.2			−2.7			−28.2				26.9	
	A	TFA	400	436		456 (s)		546	589			*i*				641	
			41.7	206.4		105.3		5.8	10.6							37.1	
chlorin dianion	MCD	NaOH	381	407	414	422		519	538	554 (s)		578[f]				610	
			2.0	6.7	−9.1	1.4		0.8	1.7	−3.5		−11.08				9.6	
	A	NaOH	394 (s)	411		433 (s)		517	543	563		581				611	
			96.5	238.4		25.0		7.2	8.2	10.4		11.6				48.4	
octaethylchlorin dianion	MCD	NaOH	390	400	410	418		520	539	555	566 (s)	583[f]				619	
			0.6	−1.5	3.6	−2.1		1.4	1.0	1.4	−1.3	−6.5				3.4	
	A	NaOH	395 (s)		414			518	545	574		587				620	
			57.1		188.5			6.5	4.7	7.9		7.8				57.0	
tetraphenylchlorin dianion	MCD	NaOH	417	428	437	446		546	568	583		613[f]				633	
			−2.0	−3.0	−3.6	6.5		0.8	−3.0	1.1		−30.3				30.5	
	A	NaOH	415 (s)	432	444 (s)			542 (s)		582		616 (s)				630	
			62.2	156.9	100.6			6.6		14.2		26.3				36.2	
octaethylbacteriochlorin	MCD	B	343	354	368 (s)			*j*				485[f]	*j*			723	
			−4.3	7.7	5.2							−16.5				3.4	
	A	B	346		375			*j*				490	*j*			724	
			168.4		180.6							32.9				154.8	
tetraphenylbacteriochlorin	MCD	B	352	363 (s)	378			*j*				523[f]	*j*			742	
			−10.2	3.9	19.1							−16.5				12.0	
	A	B	356	368 (s)	378			*j*				522	*j*			742	
			132.7	125.0	171.7							68.1				148.2	
octaethylbacteriochlorin dication	MCD	TFA	349	371	389	403	423	*j*				555[f]	*j*			776	
			−0.9	1.1	−1.4	−1.2	1.8					−4.8				2.2	
	A	TFA	348	386		404 (s)		*j*				556	*j*			775	
			72.1	102.9		81.3						16.8				46.6	
tetraphenylbacteriochlorin	MCD	TFA		366	400			*j*				617[f]	*j*			796	
dication				−2.5	8.3							−9.9				10.8	
	A	TFA		368 (s)	396			*j*				617	*j*			798	
				65.6	74.6							25.3				66.6	
zinc tetraphenylbacteriochlorin	MCD	B		356	370 (s)	389		*j*				568[f]	*j*			753	
				−5.6	4.4	11.6						−17.1				14.5	
	A	B		359	374 (s)	390		*j*				568	*j*			752	
				80.5	58.2	102.8						39.3				138.1	

Table I (*Continued*)

compound	spectrum	solvent[c]	MCD:[a] $\lambda_{max}/[\theta]_M$; absorption:[b] $\lambda_{max}/10^{-3}\epsilon$												
			Soret region				$Q_v^{x'}$				$Q_0^{x'}$[k]	$Q_v^{y'}$			$Q_0^{y'}$[k]
octaethylisobacteriochlorin	MCD	B	354	371	387			485			515[f]	552			583, *l*
			−0.8	−2.6	−4.4			1.4			2.2	3.5			−6.2
	A	B	355 (s)	370	380	401[m]		480			509	545			585, *l*
			47.8	91.1	81.7	46.8		6.3			9.2	15.9			27.9
2,2,7,7,12,13,17,18-octamethylisobacteriochlorin (8a)	MCD	B	357 (s)	368	385			482			515[f]	549			582, *n*
			−0.6	−1.9	−3.2			1.2			2.2	3.0			−5.6
	A	B	357 (s)	369	382	400[m]		480			508	542			583, *n*
			49.7	80.4	76.1	36.1		5.3			7.8	14.1			24.3
tetraphenylisobacteriochlorin	MCD	B	363	380	395	408	477	509	523	549	579[f]				600, *o*
			−2.2	−1;3	2.7	−0.6	−0.9	pos	neg	1.0	−0.4				0.3
	A	B	374 (s)	391		408 (s)	480	513		549	*i*				592, *o*
			69.2	100.0		67.5	6.8	9.2		18.0					27.7
zinc octaethylisobacteriochlorin	MCD	B	366	383	394	422					529	554			597
			2.5	2.9	−12.2	1.3					4.0	3.9			−9.5
	A	B	365	386	396	422 (s)					529	552			596
			43.1	68.9	85.6	5.9					6.3	11.5			54.7
zinc tetraphenylisobacteriochlorin	MCD	B	352	382 (s)	398	414				558	588[f]				613
			−0.4	0.6	1.2	−2.4				−0.8	−4.8				4.9
		A	365 (s)	382	403	415		489	518	556	*i*				602
			18.7	46.6	82.7	115.8		5.0	4.1	9.1					42.5
octaethylisobacteriochlorin dication	MCD	TFA	361	379	396	408					531[f]	571			608
			−1.9	0.5	1.2	−7.7					2.4	5.0			−8.9
	A	TFA		378 (s)	396	409					530 (s)	567			609
				45.8	69.2	88.2					4.4	10.7			40.4
2,2,7,7,12,13,17,18-octamethylisobacteriochlorin dication (8b)	MCD	TFA	363	378	393	407					533[f]	572			605
			−3.1	0.6	1.9	−10.7					3.4	7.2			−13.2
	A	TFA	357 (s)	376 (s)	394	409					536 (s)	564		587 (s)	608
			31.5	65.5	94.6	119.6					4.8	13.9		14.3	58.9
tetraphenylisobacteriochlorin dication	MCD	TFA		397	422	435		530			585[f]				618
				−3.3	−5.4	10.2		−2.9			−1.6				4.2
	A	TFA		403	430		510		575		*i*				614
				61.3	130.1		8.8		14.3						31.1

[a] Wavelength in nm; molar magnetic ellipticity, $[\theta]_M$, in deg cm^2 dmol^{-1} G^{-1}; s = shoulder. [b] Molar extinction coefficient, ϵ, in 1000 cm^2 mol^{-1}. [c] B = benzene; P = pyridine; TFA = 0.1 N trifluoroacetic acid in benzene; NaOH = 0.02 N NaOH in dimethyl sulfoxide–toluene–water (8:1:1 v/v/v). [d] In some cases Q_v^y bands may interdigitate in this region. [e] Some vibrational bands are not tabulated. [f] New assignments for the location of the Q_0^x transition made by MCD. [g] Contains vibrational components as well as the Q_0^x origin. The Q_0^x MCD band is probably located at 544 nm as discussed in the text. [h] The reality of two oppositely signed Q_0^y bands has been confirmed by repeated measurements in both neat pyridine and 10% pyridine in benzene. [i] Degenerate with Q_0^y absorption maximum. [j] Vibrational bands are usually weak and do not hamper assignments. [k] Symmetry axes are rotated by 45° (see Figure 1). [l] MCD: λ_{max} 637, $[\theta]_M = 0.7$; absorption: λ_{max} 636, $\epsilon = 9340$. Band attributed to the cis proton tautomer (4a-*cis*), see text. [m] Sharp absorption peak may be due to cis tautomer, see ref 47. [n] MCD: λ_{max} 637, $[\theta]_M = 0.5$; absorption: λ_{max} 634, $\epsilon = 6280$. Band attributed to cis tautomer, see text. [o] MCD: λ_{max} 655, $[\theta]_M = 0.3$; absorption: λ_{max} 653, $\epsilon = 1317$. Band attributed to tetraphenylchlorin.

siderations. First, we rely heavily on certain assignments which derive from fluorescence polarization measurements but amend and extend these assignments to chlorin derivatives for which there are no data on the basis of the MCD spectra we observe for them. Second, we assume that although the intensity of the Q_0^x transition is frequently very weak and difficult to discern as such in the absorption spectrum, the dipole strength of the transition does not vanish. Third, we recognize that both inter- and intrastate mixing mechanisms need to be allowed for in the attribution of the sign and intensity of the MCD associated with the Q_0^x transition. However, as explained in detail in Part 2,[1b] we believe that the visible region MCD spectra of chlorins is best explained on the basis that contributions[17] from the μ^+ magnetic moment dominate those of the much weaker μ^- moment. A single exception to this rule will be found in the MCD spectrum of the pyridinate adduct of zinc octaethylchlorin. Consequently, in most cases the MCD associated with the Q_0^x and Q_0^y transitions should be opposite in sign. Finally, we assume that the currently prevailing viewpoint[35] that there are only two $\pi \rightarrow \pi^*$ transitions (Q_0^x and Q_0^y) present in the visible region of chlorins is correct. Furthermore, we extrapolate a conclusion[17] from a vast body of experimental work and assume that $n \rightarrow \pi^*$ and $\sigma \rightarrow \pi^*$ transitions, if present, do not contribute significant intensity to the MCD spectrum. Consequently, we attribute the MCD intensity that is observed throughout the visible region of chlorins as being of $\pi\pi^*$ electronic or vibronic origin.

With this summary of our assignment criteria, we proceed to assign the location and to judge the MCD intensity associated with the Q_0^x transition of free-base chlorins. This will be followed by a discussion of chlorin dications and dianions and then by assignments for the zinc and zinc pyridinate complexes of the same chlorins. The section concludes with some comments on the characteristics of the transitions within the Soret envelope.

In our earlier investigation[13a] of the MCD spectra of the free-base forms of chlorins with electron withdrawing groups at the pyrrole positions, we found that the sign pattern of the MCD bands associated with the Q_0^y and Q_0^x transitions was invariably inverted, i.e., +−, respectively. In the case of the free-base chlorins studied here, there is more variety. In particular, with reference now to the Q_0^y transition, the MCD associated with this band may be of either positive (as for unsubstituted chlorin, Figure 3 and tetraphenylchlorin, Figure 5) or negative (as for octaethylchlorin, Figure 4, and bonellin, Table I) sign. In our studies with Briat[13a] the assignment of the Q_0^x transition was very straightforward since the MCD associated with it dominated that contained in vibronic bands. In the present series, the assignments are only a little less straightforward. A reliable fluorescence polarization spectrum is only available for octaethylchlorin.[37] For it, the degree of polarization of fluorescence, P^{fluor}, is about 44% at the peak of the Q_0^y absorption band, drops to about zero near 570 nm, and reaches a value of −15% at about 519 nm. These results are consistent with our assignment in Figure 4 and in Table I of the negative and positive MCD bands at 647 and 520 nm as being associated with the orthogonally polarized Q_0^y and Q_0^x transitions, respectively. The negative MCD band at about 593 nm in the spectrum of octaethylchlorin is, then, of vibronic (Q_v^y) origin. The pair of absorption bands at 487 and 496 nm are commonly considered[35,36] to be vibrational components of the Q_0^x transition. If so, they have little MCD intensity associated with them. As a final point regarding the MCD spectrum of octaethylchlorin, we note that the magnitudes of the Q_0^x and Q_0^y B terms are quite different [$B(A_0^x) = -4.1$, $B(Q_0^y) = 1.0$; in the units $D^2\,\beta_e/10^3$ cm^{-1}]. This difference may be attributable to closely spaced unresolved vibronic components in the Q_0^x band, but is more likely due to the acquisition of MCD intensity owing to the magnetically induced mixing of the Q_0^x state with a higher-energy y-polarized state, e.g., B_0^y. We will return to this point in our comments on the spectra of the zinc and zinc pyridinate complexes. The other alkyl-substituted chlorin in our series is bonellin (**5a**). It has two fewer alkyl groups than octaethylchlorin; however, it has the same sign pattern in its visible MCD bands as octaethylchlorin. Consequently, in Table I we make the same assignments for it.

In contrast to the results obtained for free-base octaethylchlorin, fluorescence polarization measurements on free-base chlorin were inconclusive.[38] A dip in the polarization spectrum was observed at 586 nm, but negative values for P^{fluor} were recorded only in the vicinity of the second putative Q_v^x absorption band at about 484 nm (Figure 3 and Table I). Since it would be expected that the presence or absence of alkyl groups at the periphery should not greatly alter the spacing between the Q_0^x and Q_0^y transitions of chlorins, either of the assignments (at 484 or 586 nm) that would follow from the fluorescence polarization measurements are suspect. Subsequent studies[39] in Shpol'skii matrices demonstrated, however, that the dip in the fluorescence polarization curve at 586 nm was due to a nontotally symmetric vibration. In the MCD spectrum of chlorin (Figure 3) this vibronic component of the Q_0^y transition is quite strong and is opposite in sign to that of the MCD of the Q_0^y transition itself. Consequently, in accordance with our criterion of oppositely signed MCD bands for the Q_0^x and Q_0^y transitions, we assign the next negative MCD band (at 510 nm) as being associated with the Q_0^x transition. The separation between the Q_0^x and Q_0^y MCD bands, then, is about 3700 cm^{-1}, which is reasonably close to that (3900 cm^{-1}) for free-base octaethylchlorin. Again, there is little MCD intensity associated with the prominent Q_v^x absorption bands. The fluorescence polarization spectrum of free-base tetraphenylchlorin does not appear to have been reported; however, similar considerations to those just outlined for chlorin and octaethylchlorin leave little doubt that the negative MCD band at 543 nm (Figure 5) is associated with the Q_0^x transition which now has considerable absorption intensity as well.

The dianions and dications of the chlorins, in distinction to the free-base derivatives, do not exhibit MCD band sign variation within the series examined here. In each case, the MCD associated with the Q_0^y transition is positive. MCD spectra for octaethylchlorin dication and tetraphenylchlorin dication are given in Figures 4 and 5, respectively. MCD data for chlorin dication, bonellin dication (**5d**) (in structure **5d**, the pyrrole substituent M

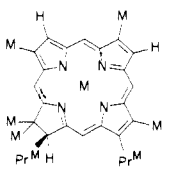

5a M = H_2
5b M = Zn
5c M = Zn Pyr
5d M = H_4^{2+}

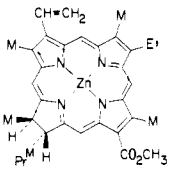

6

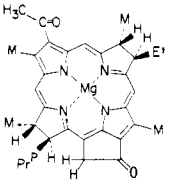

7 (P = PHYTYL)

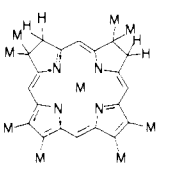

8a M = H_2
8b M = H_4^{2+}

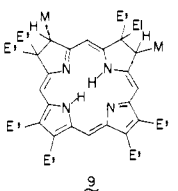

9

(37) Solovyov, K. N.; Gradyushko, A. T.; Tsvirko, M. P.; Knyukshto, V. N. *J. Lumin.* **1976**, *14*, 365–374.

(38) Sevchenko, A. N.; Solov'ev, K. N.; Mashenkov, V. A.; Shkirman, S. F. *Dokl. Akad. Nauk SSSR* **1965**, *163*, 1367–1370.

(39) Shkirman, S. F.; Solov'ev, K. N.; Arabei, S. M.; Egorova, G. D. *Izv. Akad. Nauk SSSR, Ser. Fiz.* **1978**, *42*, 658–663.

= $-CH_3$ and Pr^M = $-CH_2CH_2CO_2CH_3$), and all of the dianions are collected in Table I. Fluorescence polarization data are not available for any of the chlorin dianions or dications, but assignments for the location of the Q_0^x transition can be deduced from their MCD spectra in conjunction with some precepts of the four-orbital model. Gouterman notes,[30a] and collects supporting data from the absorption spectra of metal tetraphenylchlorins, that the b_1 orbital of chlorins should rise in energy with increasingly electropositive metals. In the present series, the metals are the four protons of the dication, the two sodium ions of the dianion, and zinc. As a result of this shift in the level of the b_1 orbital, the Q_0^x and Q_0^y transitions should become more closely spaced. This coalescence of transition energies is also reflected in the MCD spectrum. For example, in the spectra of the tetraphenylchlorins (Figure 5), the oppositely signed MCD bands associated with the Q_0^x and Q_0^y transitions of zinc tetraphenylchlorin (vide infra) have the distinct appearance of two closely spaced *B* terms. On the other hand, in the MCD spectrum of tetraphenylchlorin dication the Q_0^x and Q_0^y MCD bands straddle the main absorption band maximum and thus have the general appearance of an *A* term. In the absorption spectrum, the half-bandwidth of the strong absorption band is about three times that of the zinc complex and it is clear that the Q_0^x and Q_0^y transitions of tetraphenylchlorin dication have become accidentally degenerate. In the case of octaethylchlorin dication (Figure 4) the Q_0^x and Q_0^y transitions are more widely separated and the MCD bands associated with these transitions appear as well-defined *B*-term-type bands. In the unsubstituted and alkyl- and tetraphenylchlorin dications and dianions some MCD intensity is found in the vibronic bands; however, this occurrence does not obscure our assignments in Table I of the second strong negative MCD band as being associated with the Q_0^x transition.

Substituent-induced MCD band sign variation within the present series of chlorins is again found for the zinc and zinc pyridinate complexes. Spectra for the zinc complexes of chlorin, octaethylchlorin, and tetraphenylchlorin are shown here in Figures 3, 4, and 5, respectively, and the spectra of the pyridinate complexes of zinc chlorin, zinc octaethylchlorin, and zinc bonellin are directly compared with those of the corresponding unligated species in Figures 6, 7, and 8, respectively, of Part 2.[1b] The occurrence of MCD band sign inversion in the unligated zinc complexes parallels its occurrence in the free-base derivatives—the Q_0^y MCD band is positive for zinc chlorin and zinc tetraphenylchlorin but negative for zinc octaethylchlorin and zinc bonellin. Formation of the five-coordinate pyridinate complexes results in an increase in the intensity of the positive Q_0^y MCD band of zinc chlorin, causes the Q_0^y MCD band of zinc bonellin to change sign from negative to positive, and in the case of zinc octaethylchlorin, gives rise to a pair of weak oppositely signed MCD bands. The elaboration of Michl's perimeter model in Part 2 provides a nice rationale for these and other substituent-induced MCD band sign variations in the chlorin series.

Fluorescence polarization spectra have been reported for zinc octaethylchlorin[40] and zinc tetraphenylchlorin.[41a] The assignment of the Q_0^x transition of zinc tetraphenylchlorin is definitive since P^{fluor} is close to 50% at the absorption maximum of the strong red band and almost reaches the theoretical limit of −33% at the peak of the second absorption band. In the MCD spectrum of zinc tetraphenylchlorin (Figure 5), this assignment translates to the first negative MCD band at 586 nm as being the Q_0^X MCD band. The second negative MCD band at 555 nm is assigned as Q_v^x. The fluorescence polarization technique is much less definitive in the case of zinc octaethylchlorin since P^{fluor} does not reach negative values at any point in the visible region; however, Gradyushko et al.[40] place the Q_0^x transition at 544 nm. MCD is much more useful in this respect because of the almost stringent criterion that the MCD bands associated with the Q_0^x and Q_0^y transitions be of opposite sign. Consequently, we assign the positive MCD band at 538 nm in the spectrum of zinc octaethylchlorin (Figure 4) as the band associated with the Q_0^x transition and accord the negative bands at 561 (s) and 573 nm as being of vibronic (Q_v^y) origin. An analogous assignment is entered in Table I for zinc bonellin (**5b**). The MCD spectrum of zinc rhodochlorin (**6**) which was given in Figure 1 of our preliminary communication[1a] provides an interesting contrast to that of zinc octaethylcholorin (Figure 4) since, as will be discussed in Part 2,[1b] the MCD associated with its Q_0^x and Q_0^y transitions are inverted owing to the presence of vinyl and methoxycarbonyl groups in rings I and III. For it, we assign the second negative MCD band at 555 nm to the Q_0^x transition. This is consistent with the fluorescence polarization spectrum recorded for the structurally similar chlorophyll derivative, zinc pheophytin *a*.[41b]

The assignment of the Q_0^x MCD band for the parent chromophore, zinc chlorin, is somewhat more tenuous. No assistance can be garnered from fluorescence polarization as was the case for the other zinc chlorins since Sevchenko et al.,[41a] in referring to their measurement of its spectrum, stated that the location of the Q_0^x transition could not be determined, owing, presumably, to its low intensity. A similar problem was encountered in the fluorescence polarization spectrum of free-base chlorin;[38] however, we found (vide supra) that the location of its Q_0^x transition could be unequivocally assigned from the MCD spectrum. In the MCD spectrum of zinc chlorin (Figure 3), we reject the most transparent assignment for the Q_0^X MCD band as being the strong negative MCD band at 567 nm; instead, we assign the 567-nm band as a vibronic component of the Q_0^y transition. This attribution is consistent with our previous assignments for the similarly located negative MCD band in the spectra of zinc octaethylchlorin (Figure 4) and zinc bonellin (Table I). We assign (in Figure 3 and in Table I) the negative peak at 555 nm on the blue side of the strong Q_v^y MCD band system as the Q_0^x MCD band of zinc chlorin. The absorption spectrum of zinc chlorin does not show a clear maximum in this region and no corresponding entry is made in Table I. The positive MCD bands at somewhat higher energies are, then, assigned as vibronic components of the Q_0^x transition.

The assignment of the actual location of the Q_0^x transition for the zinc and zinc pyridinate complexes of chlorins, especially those with alkyl substituents, requires some additional comments on the ways in which the MCD bands of these, and the other reduced porphyrins, may acquire intensity.

In its usual truncated form,[12a,17a] the expression for the *B* term is the sum over relevant states of the scalar triple product of the electric dipole transition moments which connect the ground and two excited states and the magnetic dipole transition moment which connects two excited states. The denominator contains the difference in energies of the two excited states relative to the ground state. Consequently, the magnetic moments involved, the dipole strengths of the electronic transitions, and their separations in energy are all important factors to be considered. In the context of the four-orbital model, the Q_0^y transition acquires most of its MCD intensity through mixing with the Q_0^x transition rather than with the more distant B_0^x transition. The Q_0^x transition of free-base chlorins, however, is well separated from the Q_0^y transition and may aquire MCD intensity by mixing with both the B_0^y and Q_0^y transitions. In the case of octaethylchlorin, for example, the spacing between the Q_0^x and Q_0^y transitions is 3770 cm^{-1}, whereas the spacing between the Q_0^x transition and the peak of the Soret absorption band is 6280 cm^{-1}. Thus, notwithstanding the greater difference in energy, the larger dipole strength of the B_0^y transition combined with a nonzero magnetic moment can allow the Q_0^x MCD band to acquire additional intensity. Since the vibronic components of the Q_0^x transition of octaethylchlorin evidently have little MCD associated with them (Figure 4), we used (*vide supra*) this mechanism to account for the fourfold difference in the magnitude of the Q_0^x and Q_0^y *B* terms.

The zinc complexes of the chlorins present a somewhat different picture. In the case of zinc octaethylchlorin, the separation between the MCD bands we associate with the Q_0^x and Q_0^y tran-

(40) Gradyushko, A. T.; Solov'ev, K. N.; Tsvirko, M. P. *Opt. Spektrosk.* **1978**, *44*, 1123–1130.

(41) (a) Sevchenko, A. N.; Solov'ev, K. N.; Mashenkov, V. A.; Shkirman, S. F.; Losev, A. P. *Dokl. Akad. Nauk SSSR* **1967**, *175*, 797–799. (b) Dvornikov, S. S.; Knyukshto, V. N.; Sevchenko, A. N.; Solovev, K. N.; Tsvirko, M. P. *Sov. Phys. Dokl. (Engl. Transl.)* **1978**, *23*, 748–750.

sitions is 2330 cm^{-1}, whereas the separation between the Q_0^x MCD band and the peak of the Soret absorption band is 6410 cm^{-1}. On this basis, even assuming roughly the same magnetic moments and dipole strengths for the free base and for the zinc complex, the amount of MCD intensity garnered by the Q_0^x transition through mixing with the B_0^y transition should be less for the zinc complex than for the free base. However, for zinc octaethylchlorin $B(Q_0^x) = -5.2$, whereas $B(Q_0^y) = 1.3$ (in the units $D^2\beta_e/10^3$ cm^{-1}). In addition to interstate mixing, another source of intensity for the MCD band labeled as Q_0^x in the spectrum of zinc octaethylchlorin (Figure 4) is through the overlapping of vibronic components which have appreciable positive MCD intensity. The basic reality of this proposition can be seen in the MCD spectrum of zinc chlorin (Figure 3). Here, the sign of the Q_0^x MCD band is negative (the peak at 555 nm) but its vibronic components have positive signs.

Further support for the general attribution of significant MCD intensity for the Q_v^x transitions of metal chlorins comes, for example, from the MCD spectrum of zinc tetraphenylchlorin (Figure 5). In this case, the intensity of the now negatively signed Q_v^x MCD band at about 555 nm is relatively strong.

The wavelength shifts and the sign inversions that occur in the MCD spectra of some of the zinc complexes on ligation with pyridine provide an additional perspective to the question of vibronically induced MCD intensity. These changes also aid in the assignment of the location of the Q_0^x transition of these complexes. This is important in the context of the discussions in Part 2[1b] where we assert that the unsubstituted and alkyl-substituted chlorins are apposite examples of an "almost soft" MCD chromophore. A rough estimate of the red shift that occurs in the Q_0^x transition of zinc chlorins on ligation with pyridine can be obtained from the spectral data for the tetraphenylchlorin derivatives given in Table I. In the unligated zinc complex, the Q_0^x MCD band is at 586 nm; in the ligated derivative the band is at 600 nm. This corresponds to a red shift of the Q_0^x MCD band, and thus the Q_0^x transition, of at least 14 nm (400 cm^{-1}). A similar coalescence of the Q_0^x and Q_0^y transitions, owing to the rise in the energy of the b_1 orbital on ligation (Figure 3, Part 2[1b]), is expected and is observed for zinc chlorin, zinc octaethylchlorin, and zinc bonellin (see Figures 6, 7, and 8, respectively, in Part 2[1b]). It is more difficult, however, to estimate the red shift of the Q_0^x transition in these cases because of the occurrence of sign inversions and because of the MCD intensity which seems to generally prevail in the Q_v^y transitions.

For example, in the case of zinc bonellin (Figure 8, Part 2[1b]), the sign of the Q_0^y MCD band changes from negative to positive on going to the pyridinate complex. We anticipate, for the reasons stated at the beginning of this section, that the MCD band associated with the Q_0^x transition should have the opposite (negative) sign. Positive MCD intensity does, however, remain in the region of the MCD band which we have previously assigned as being associated with the Q_0^x transition of the unligated species. We infer from this that, in addition to interstate mixing, a significant portion of the positive intensity in the MCD band labeled Q_0^x of the unligated zinc complex comes from unresolved vibronic components. If true, this would also suggest that the actual position of the Q_0^x MCD band of the unligated zinc complex is located under the red edge of the main positive MCD band at 537 nm in the spectrum of zinc bonellin. Recall that the fluorescence polarization spectrum of zinc octaethylchlorin[40] suggested that the Q_0^x transition was at 544 nm.

A way of estimating the location of the Q_0^x transition in the ligated species is either to use the 400-cm^{-1} shift observed for zinc tetraphenylchlorin or to assume that the vibronic components of the Q_0^x transition of zinc bonellin red shift rigidly along with the Q_0^x transition. We use, for the latter case, the shifts in the weaker positive Q_v^x bands around 500 nm in the spectra of zinc bonellin (Figure 8, Part 2[1b]). The shift in their positions on ligation is 310 cm^{-1}. If the Q_0^x transition of zinc bonellin lies under the red edge of the main positive MCD band and is at about 544 nm, then the Q_0^x transition of the pyridinate complex should be identified with the negatively signed shoulder at about 560 nm rather than with the more intense negatively signed MCD band at 576 nm which we assign as being of Q_v^y origin. The same conclusion is reached when the zinc tetraphenylchlorin shift is used. Since zinc moves out of the plane of the macrocycle on formation of five-coordinate complexes, it is not surprising that some additional changes occur in the intensities of the vibronic MCD bands.

A similar line of reasoning can be applied to the spectra of the unligated and ligated forms of zinc octaethylchlorin (Figure 7, Part 2[1b]). The spectrum of the pyridinate complex of zinc octaethylchlorin is, however, distinguished from that of zinc bonellin by the fact that the integrated intensity of the Q_0^y MCD band is zero. The actual band shape consists of two oppositely signed MCD bands. This suggests to us, as will be advocated in Part 2,[1b] that the pyridinate complex of zinc octaethylchlorin closely approximates the "soft" MCD chromophore case[17b] where $\Delta HOMO = \Delta LUMO \neq 0$. The intensity in the MCD band at 566 nm which we assign to the Q_0^x transition may arise in part from μ^- magnetic moment contributions, whereas in the other chlorins it has been necessary to consider only the contributions from the μ^+ moment. The MCD spectrum of the pyridinate complex of zinc chlorin (Figure 6, Part 2) shows two oppositely signed MCD bands of equal $|[\theta]_M|$ (Table I). In our interpretation of the spectra of the other zinc chlorins, we have attributed the first negative MCD band to a vibronic component of the Q_0^y transition. In this particular case, recalling that our value of 310 or 400 cm^{-1} for the pyridine-induced red shift is probably somewhat underestimated, we assign the strong negatively signed band at 573 nm as the Q_0^x MCD band. Vibronic components of the Q_0^y transition, however, do account for the pair of negatively signed MCD bands at about 554 nm.

In order to derive coherent structural information from the sign patterns of the MCD bands in the Soret region of porphyrins and reduced porphyrins with Michl's perimeter model,[17] it is necessary that there be only two electronic transitions within the Soret envelope and that transitions to higher-lying states be well separated from it. Fluorescence polarization measurements support the two-state requirement. For free-base chlorin[38] and octaethylchlorin[37] the polarization spectra are consistent with the ordering: B_0^y, B_0^x with increasing energy. In the case of zinc tetraphenylchlorin[41a] and zinc octaethylchlorin,[40] the ordering inferred from their spectra is B_0^y, B_0^x and B_0^x, B_0^y, respectively. MCD, on the other hand, indicates that the composition of the Soret absorption envelope is more complex. For example, in the MCD spectrum of zinc tetraphenylchlorin (Figure 5) it appears that there are two electronic transitions, whereas in the free base there may be as many as five or six. An additional complicating factor for structure–spectra correlations (Part 2) is that the signs of the lowest energy MCD bands in the visible and in the Soret regions do not always correspond. This can be seen in the spectra of the tetraphenylchlorin derivatives. These conclusions about the actual complexity of the composition of the Soret absorption band as judged by MCD are supported by the recent ab initio calculations on chlorins by Petke et al.[35] They find for free-base chlorin five moderate-to-strong $\pi \rightarrow \pi^*$ transitions with the lowest one having y polarization. In the case of magnesium chlorin, four $\pi\pi^*$ states are responsible for most of the intensity of the Soret band with the one of lowest energy having x polarization.

(ii) Bacteriochlorins. In contrast to the chlorins, the vibrational bands in the visible region of octaethyl- and tetraphenylbacteriochlorin have little MCD intensity associated with them, and the assignments made for the Q_0^x and Q_0^y MCD bands of the free base, dications, and zinc complexes of these two compounds in Figures 6 and 7 and in Table I follow without difficulty. Polarization measurements do not seem to have been reported for any synthetic bacteriochlorin; however, fluorescence polarization and linear dichroism spectra have been reported for bacteriochlorophyll *a* (7) itself.[42,43] The room-temperature fluorescence polarization spectrum of 7 in caster oil[42] is not sharply defined

(42) Ebrey, T. G.; Clayton, R. K. *Photochem. Photobiol.* **1969**, *10*, 109–117.
(43) Bauman, D.; Wrobel, D. *Biophys. Chem.* **1980**, *12*, 83–91.

but definitely shows that the transitions at about 760 and 590 nm have opposite polarization. The MCD spectrum of bacteriochlorophyll[14] in ether is unequivocal in locating the Q_0^y and Q_0^x bands at 770 and 573 nm, respectively. The wavelength shifts from those we observe for octaethylbacteriochlorin dication (Figure 6) are largely due to the presence of carbonyl substituents in rings I and III of **7**. In MCD the inverted sign pattern is observed with the lowest-energy Soret and visible bands being of the same sign in all of the bacteriochlorin derivatives examined. The ab initio calculations of Petke et al.,[44] on ethyl bacteriochlorophyllide *a* and ethyl bacteriopheophorbide *a* (the free base) indicate that, while transitions to a number of states appear in the Soret region, the composition of the high-intensity ones is strongly "four orbital" in nature. The lowest-energy Soret transition in both cases is calculated to have *x* polarization. Taken together, our MCD and absorption spectra (Figures 6 and 7 and Table I) indicate the presence of three strong transitions just within the two-peaked region of the Soret envelope.

(iii) Isobacteriochlorins. The assignment of the Q_0^x transition[45] in the spectra of octaethylisobacteriochlorin (Figure 8 and Table I) and 2,2,7,7,12,13,17,18-octamethylisobacteriochlorin (**8**)[46] (Table I) cannot be made with certainty from their MCD spectra alone since they both exhibit two strong positive MCD bands in the spectral region, 480–560 nm, where the Q_0^x transition would be expected. However, the fluorescence and fluorescence polarization spectra reported[40] for zinc octaethylisobacteriochlorin clearly identify the third absorption band as the Q_0^x transition. In the MCD spectrum of this compound (Figure 8), this assignment correlates with the second positive MCD band at about 529 nm. Since the MCD in the visible region of the free base and dication derivatives are very similar to that of the zinc complex, we make the same assignments for them. This assignment is extended to Eschenmoser's[46] isobacteriochlorin (**8**) in Table I. The positive MCD band at about 550 nm in the spectra of the alkyl isobacteriochlorin derivatives is, then, taken to be a vibrational band of Q_0^y origin. Vibronic components of the Q_0^x band are probably responsible for the positive MCD found below about 500 nm.

Initially, the assignment of the positive MCD band at 637 nm in the spectrum of octaethylisobacteriochlorin (Figure 8) was puzzling since, if it had been due to an octaethylchlorin impurity, then the sign of the MCD band should have been negative and at 647 nm (Figure 4). This problem seems now to have been resolved by the recent work of Chang[47a] on another synthetic alkyl-substituted isobacteriochlorin, **9**. The infrared and low-temperature absorption spectra of **9** suggested that in solution an equilibrium between the cis and trans proton tautomers of isobacteriochlorins may exist as shown below. The trans tautomer, which has a formally interrupted conjugation path, is considered by Chang to be the more stable species largely on the basis of the severe steric interactions between the hydrogens that should be present for the cis tautomer. Chang's low-temperature measurements indicate that the sharp band at 400 nm and the band at 637 nm in the room-temperature absorption spectrum of octaethylisobacteriochlorin (Figure 8) are due to the cis tautomer. In order to judge the contributions of the tautomers to the MCD spectrum, we have measured the room-temperature and 77 K MCD spectra of octaethylisobacteriochlorin in EPA. From a comparison of the two spectra shown in Figure 9, it is clear that the long-wavelength MCD band does indeed disappear at low temperature. There is also a loss of MCD intensity in the 400–500-nm region. In the Soret region the second, and negative, MCD band decreases in intensity and a new positive MCD band appears. Elsewhere, the shape of the MCD spectrum remains essentially the same as at room temperature. There is little MCD intensity associated with the sharp 400 nm absorption band.

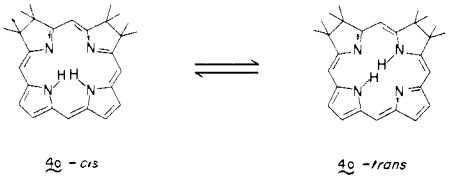

The tetraphenylisobacteriochlorins (Figure 10, Table I) present an entirely different MCD picture as compared to the alkyl-substituted isobacteriochlorins with regard to the location of the visible transitions and the sign of the MCD associated with them. In the spectra of zinc octaethylisobacteriochlorin (Figure 8) the positions of the MCD and absorption bands assigned to the Q_0^y transition are essentially coincident and the sign of the Q_0^y MCD band is negative. In the MCD spectrum of zinc tetraphenylisobacteriochlorin (Figure 10) there are only two strong visible MCD bands and the sign of the lowest-energy one, the Q_0^y band, is positive. These bands, positive at 613 nm and negative at 588 nm, straddle the main visible absorption band at 602 nm. In the MCD spectrum of tetraphenylisobacteriochlorin dication (Table I) the MCD bands also straddle the absorption band at 614 nm but there is relatively less intensity in the negative MCD band. In the free base the positive and negative MCD bands at 600 and 579 nm, respectively, are much weaker than in the zinc complex but still straddle the main visible absorption band at 592 nm. This similarity in the disposition of the electronic absorption and MCD bands in the free base, dication, and zinc complex of tetraphenylisobacteriochlorin strongly suggests that the Q_0^x and Q_0^y transitions of each are accidentally degenerate and underly the lowest-energy visible absorption band. In the alkyl-substituted isobacteriochlorins, these transitions were much more widely spaced.

The MCD spectrum of tetraphenylisobacteriochlorin also contains a small positive "extra" band at 655 nm. While this band could arise from a proton tautomer, as for octaethylisobacteriochlorin, it did not decrease in intensity at 77 K, and we consider that it is due to a small (1.5%) tetraphenylchlorin impurity which does not otherwise make a significant contribution to the rest of the spectrum of the tetrahydro derivative.

Ab initio calculations on an isobacteriochlorin have not been carried out.[48] Consequently, an evaluation of the four-orbital model's representation of the Soret band of isobacteriochlorins on the same basis as was made above for porphyrins, chlorins, and bacteriochlorins is not possible. However, according to the PPP calculations of Weiss[49] the B bands of metal isobacteriochlorin are 87% and 95% derived from four-orbital states with the lowest-energy one having *x* polarization. The fluorescence polarization spectrum of zinc octaethylisobacteriochlorin[40] shows negative polarization on the red edge of the Soret band and is thus consistent with Weiss's assigned ordering. In general, our MCD and absorption spectra for the isobacteriochlorins are consistent with the presence of at least three transitions within the Soret envelope. The lowest-energy strong Soret and visible MCD bands of the free base, dication, and zinc salt derivatives of the alkyl-substituted isobacteriochlorins (Figure 8 and Table I) have the same sign. This pattern is not consistently maintained in the tetraphenylisobacteriochlorin series (Figure 10 and Table I).

Summary

In Part I of our investigation of the MCD of chlorins, bacteriochlorins, and isobacteriochlorins, we have made a number

(44) Petke, J. D.; Maggiora, G. M.; Shipman, L. L.; Christoffersen, R. E. *Photochem. Photobiol.* **1980**, *32*, 399–414.

(45) In Table I and Figures 8 and 10 we label the Q_0^x and Q_0^y transitions of the isobacteriochlorins as $Q_0^{x'}$ and $Q_0^{y'}$ in recognition of the rotation of the symmetry axes by 45° (Figure 1) but omit the prime in the text.

(46) Monforts, F. P.; Ofner, S.; Rasetti, V.; Eschenmoser, A.; Woggon, W. D.; Jones, K.; Battersby, A. R. *Agnew. Chem., Int. Ed. Engl.* **1979**, *18*, 675–677.

(47) (a) Chang, C. K. *Biochemistry* **1980**, *19*, 1971–1976. (b) Chang, C. K.; Hanson, L. K.; Richardson, P. F.; Young, R.; Fajer, J. *Proc. Natl. Acad. Sci. U.S.A.* **1981**, *78*, 2652–2656.

(48) Maggiora, G. M., personal communication.

(49) Weiss, C., Jr. *J. Mol. Spectrosc.* **1972**, *44*, 37–80.

of new assignments for the location of the Q_0^x transition. The assignments for some of the chlorins are somewhat equivocal because of the presence of vibrational bands with appreciable MCD intensity.

Michl's prediction[17b] of the inverted, +−+−, sign pattern for the visible and Soret MCD bands of bacteriochlorins is confirmed. In the chlorin series, we find that the specific sign pattern observed is remarkably sensitive to the particular substituents on the periphery and at the center of macrocycle. In free-base chlorin, for example, the visible but not the Soret MCD bands are inverted, whereas in octaethylchlorin the visible and Soret MCD bands show the normal, −+−+, sign pattern. In zinc octaethylchlorin the sign pattern is normal while in octaethylchlorin dication the inverted pattern is again seen. In the isobacteriochlorin system Michl[17b] concluded that $\Delta HOMO \approx \Delta LUMO$ and did not explicitly predict the sign pattern. Our MCD spectra show that the MCD sign pattern for the Q_0^x and Q_0^y transitions in the alkyl-substituted isobacteriochlorin derivatives is normal, whereas in the tetraphenylisobacteriochlorin derivatives the sign pattern is inverted. In the Soret region the sign pattern does not always follow that in the visible.

In conclusion, we believe that our results are highly pertinent to spectroscopists, chemists, and biochemists involved in the study of reduced porphyrins since they provide an adequate experimental demonstration that the MCD sign patterns of these systems depend, in general, on the substituents present. In Part 2[1b] we elaborate Michl's perimeter model[17] and show how our results can be rationalized and how further predictions can be made.

Acknowledgment. We wish to thank Professors A. Eschenmoser and A. Pelter for providing samples of 2,2,7,7,12,13,17,18-octamethylisobacteriochlorin and bonellin, respectively. We also thank Professor R. H. Holm for his interest in this project and Ruth Records for her assistance with measurements. Y.-C.L. was a visiting scholar from the Beijing Institute of Chemical Reagents. A.M.S. was a predoctoral fellow of the Fannie and John Hertz Foundation. Financial support of this research was provided by grants from the National Science Foundation (CHE-77-04397 and CHE-80-09240) and the National Institutes of Health (GM-20276 and HL-16833).

Registry No. 1a, 101-60-0; **2a**, 2683-84-3; **5a**, 82113-29-9; **5b**, 75214-81-2; **5c**, 82135-12-4; **5d**, 82166-55-0; **6**, 78023-42-4; **8a**, 71250-54-9; **8b**, 82113-30-2; *trans*-octaethylchlorin, 22862-60-8; tetraphenylchlorin, 13554-17-1; zinc chlorin, 77124-66-4; zinc octaethylchlorin, 28375-45-3; zinc tetraphenylchlorin, 14839-32-8; zinc chlorin pyridinate, 82135-09-9; zinc octaethylchlorin pyridinate, 82135-10-2; zinc tetraphenylchlorin pyridinate, 82135-11-3; chlorin dication, 82113-31-3; octaethylchlorin dication, 82113-32-4; tetraphenylchlorin dication, 50849-36-0; chlorin dianion, 55309-59-6; octaethylchlorin dianion, 38705-82-7; tetraphenylchlorin dianion, 82113-33-5; octaethylbacteriochlorin, 23016-64-0; tetraphenylbacteriochlorin, 5143-18-0; octaethylbacteriochlorin dication, 82113-34-6; tetraphenylbacteriochlorin dication, 82113-35-7; zinc tetraphenylbacteriochlorin, 50795-70-5; octaethylisobacteriochlorin, 72260-12-9; tetraphenylisobacteriochlorin, 25440-13-5; zinc octaethylisobacteriochlorin, 39001-89-3; zinc tetraphenylisobacteriochlorin, 14705-64-7; octaethylisobacteriochlorin dication, 82113-36-8; tetraphenylisobacteriochlorin dication, 82113-37-9; zinc porphine, 14052-02-9.

Magnetic Circular Dichroism Studies. 61. Substituent-Induced Sign Variation in the Magnetic Circular Dichroism Spectra of Reduced Porphyrins. 2. Perturbed Molecular Orbital Analysis[1]

Joseph D. Keegan, Alan M. Stolzenberg, Yu-Cheng Lu, Robert E. Linder,[2] Günter Barth, Albert Moscowitz,*[3b] Edward Bunnenberg, and Carl Djerassi*[3a]

Contribution from the Departments of Chemistry, Stanford University, Stanford, California 94305, and The University of Minnesota, Minneapolis, Minnesota 55455.
Received October 21, 1981

Abstract: The MCD data in Part 1 for a series of unsubstituted, alkyl-substituted, and tetraphenyl-substituted chlorins, bacteriochlorins, and isobacteriochlorins are subjected to a perturbed molecular orbital analysis in order to test the utility and applicability of Michl's perimeter model for relating the absolute signs of the four lowest-energy purely electronic MCD bands of cyclic π-electron systems to their molecular structures. A protocol is developed for this purpose which does not require explicit numerical calculations, but instead combines the elements of an experimental basis and the classic concepts of Gouterman's four-orbital model of porphyrin states in order to estimate the relative absolute size of the orbital energy differences between the two highest occupied ($\Delta HOMO$) and the two lowest unoccupied ($\Delta LUMO$) molecular orbitals. In the isobacteriochlorin series the splitting in the LUMO's evident from MO calculations is included in the protocol in an ad hoc manner. The MCD band sign patterns of all porphyrins and reduced porphyrins investigated are correctly predicted with the use of our protocol in conjunction with Michl's model. Particular emphasis is placed on the subtle peripheral and central substituent-induced sign variations which occur in the chlorin series. The application of the model as a useful first-order structural-elucidation technique for other systems is illustrated by reference to some naturally occurring reduced porphyrins.

The occurrence of sign and intensity variations in the magnetic circular dichroism (MCD) spectra of a series of related organic molecules suggests the possibility of developing a theoretical framework from which relatively simple rules can be elicited for relating molecular structures to their observed spectra. In our own early work we found a variety of signs, shapes, and intensities for the MCD associated with the $n \rightarrow \pi^*$ transition of saturated ketones.[4a] In later work we developed a protocol for extracting

(1) For Part 60, see the preceding paper in this issue.
(2) Surface Science Laboratory, 4151 Middlefield Road, Palo Alto, California 94303.
(3) (a) Stanford University. (b) University of Minnesota.

0002-7863/82/1504-4317$01.25/0